ISTITUTO NAZIONALE DI FISICA NUCLEARE

Sezione di Milano

INFN/TC-83/15
20 Settembre 1983

G. Barbiellini, G. Cecchet, J. Y. Hemery, F. Lemeilleur, P. G. Rancoita, A. Seidman and M. Zilka: SILICON/TUNGSTEN CALORIMETER AS LUMINOSITY MONITOR

Servizio Documentazione
dei Laboratori Nazionali di Frascati

Istituto Nazionale di Fisica Nucleare
Sezione di Milano

INFN/TC-83/15
20 Settembre 1983

G. Barbiellini[1], G. Cecchet[2], J. Y. Hemery[3], F. Lemeilleur[3], P. G. Rancoita[4], A. Seidman[5] and M. Zilka[5]:

SILICON/TUNGSTEN CALORIMETER AS LUMINOSITY MONITOR

Contributed paper no. 102 to the "International Europhysics Conference on High Energy Physics", Brighton, 20-27 July, 1983

(Presented by P. G. Rancoita).

ABSTRACT

A compact electromagnetic calorimeter is provided by a sandwich of high-Z material (like tungsten) and silicon detectors as active sampling layers. Inexpensive detectors are obtained by employing relative low-resistivity material and work as undepleted devices. The associated electronics oriented to high input capacitances has shown the appropriate performance. The measurement of the small-angle Bhabha scattering can provide a luminosity monitor for e^+e^- beam colliding machines. The energies and the directions of flight of the scattered electron and positron can be measured by a silicon tungsten calorimeter and a set of microstrip detectors. In order to get a relatively high counting rate it should be located as close as possible to the beams.

---

[1] Laboratori Nazionali dell'INFN, Frascati, and CERN, Geneva, Switzerland

[2] INFN - Sezione di Milano and INFN - Sezione di Pavia

[3] CERN, Geneva, Switzerland

[4] INFN - Sezione di Milano (present address: CEN, Saclay, France)

[5] Tel-Aviv University, Ramat-Aviv, Israel

1. - INTRODUCTION

The luminosity monitor for e^+e^- beam colliding machines is provided by the measurement of the Bhabha scattering ($e^+e^- \rightarrow e^+e^-$)[1]. In the very forward direction the square momentum transfer $q^2 \approx E^2\theta^2$ (E is the beam energy and θ the scattering angle) is much smaller than Γ_Z^2 (Γ_Z is the Z^o width). Thus the elastic cross-section at small scattering angle is given by

$$d\sigma/d\Omega \approx 4r_o^2(mc^2/E)^2(1/\theta^4)$$

where r_o is the classical radius of the electron and m the electron mass.

A large rate $n = L\sigma$ (L is the machine luminosity and σ is the cross-section) is obtainable if the scattered electrons (and positrons) are detectable at sufficiently small angles. At $\theta \approx 10$ mr and $E \approx 50$ GeV, few elastic events per second are produced for $L \approx 10^{31}$ cm^2s^{-1}. This way fast feedback is provided at a change in the machine parameters compared with those for the optimal bunch overlap.

The elastic scattering events are detected by a coincidence of two back-to-back electrons, each one carrying the beam energy. Therefore, the luminosity monitor should be able to track the electron and positron and to measure their energies. The tracking device can be provided by a set of microstrip detectors, which are widely used in high-energy physics[2]. Sandwich of large-size silicon detectors and tungsten provides electromagnetic calorimetry by a high compact detector. For this purpose relatively inexpensive low-resistivity silicon can be used. In calorimetry a small depleted volume ($\approx$ 50% of the physical one) is sufficient since the number of particles to be detected is quite large.

2. - APPLICATION OF SILICON DETECTORS TO CALORIMETRY

Silicon detectors can find application in calorimetry. They operate in strong magnetic fields, are manufactured following dedicated design and work in vacuum enviroment. Their associated electronics can be easily accomodated nearby. However their main advantage is the higher density compared with those of other active sampling materials[3].

In high-energy physics experiments, silicon detectors have been employed to detect relativistic particles. However their number was always limited. In calorimetry, however, silicon detector in large numbers, and with large active areas are employed.

Inexpensive devices[4] can be produced to be i) operated at low voltage (50-60 V), ii) made of relatively low resistivity material (1000-1500 Ωcm), and iii) cut to standard thickness of 250-300 μm. These devices are supposed to operate as large active area, high capacitance and undepleted detectors.

2. 1. - Silicon detector and calorimeter energy resolution

The luminosity monitor can be built (sect. 3.1) by employing the silicon detectors as active sampling layers.

The calorimeter length(5) needed to contain the 98% of the incoming electron energy up to 50 GeV is about 24-28 radiation lengths. By using tungsten as showering material about 95% of the total energy(6) is contained in a cylinder of radius $R \approx 1.8$ cm.

The sampling fluctuations dominate in a calorimeter with dense active silicon layers and the expected energy resolution is(6)

$$\sigma(E)/E \approx 3.2\% \sqrt{\left[\varepsilon(\mathrm{MeV})/F(z)\cos(E_s/\pi\varepsilon)\right]} \sqrt{\left[t/E(\mathrm{GeV})\right]}$$

where $F(z) \approx 0.9$, $E_s \approx 21$ MeV, ε (the critical energy for tungsten) ≈ 7.6 MeV and t is the thickness of the showering material in unit of radiation length.

2. 2. - Undepleted silicon detectors

A silicon detector operates in reverse biased condition, namely the applied voltage assists the built-in voltage in removing free charges from the junction interface and the regions on either side of it. It is here, in the so-called depletion layer where the free carrier concentrations are below their thermal equilibrium values, that the conditions for counter operation can exist. Thus the holes and electrons (h-e) created subsequently to the energy-loss process can migrate towards the electrodes.

To a first approximation, the distance d to which the depletion layer penetrates is

$$d \propto \sqrt{(V + V_o)}$$

where V_o is the build-in voltage and V the applied reverse bias. For $V > V_o$ and n--type silicon, we have

$$d \approx 0.53 \sqrt{(\varrho V)} \qquad (\mu m)$$

where ϱ is the resistivity in Ωcm, V is the reverse bias in Volts. The extension of the depletion region can be estimated also by measuring the detector capacitance. For an n-type silicon, the capacitance per unit area is

$$c \approx 1.17 \times 10^4 \, d^{-1} \qquad (\mathrm{pF/cm^2})$$

where d is the depleted layer in μm. The transit time is

$$\tau_t = d/(\mu E)$$

and for an undepleted n-type silicon detector

$$\tau_t \approx 5.6 \times 10^{-3} \varrho \quad \text{(ns)}.$$

As an example, a relatively inexpensive detector with a resistivity of $\approx 1500\ \Omega$cm, manufactured with a standard thickness of 300 μm and operated at a reverse bias of 60 V, has a depleted region of $\approx 160\ \mu$m, a capacitance of ≈ 73 pF and transit time of ≈ 8 ns.

In actual practice the sensitive region of an undepleted detector is the charge-depletion layer plus an additional region, the thickness of which is a fraction of a carrier-diffusion length[7]. In fact few charges can diffuse into the space-charge region from the field-free region. By neglecting the recombination and considering only the charge diffusion, we can estimate the upper limit of charge migration towards the space-charge region. In the field-free zone the diffusion equation for holes (minority carriers in an n-type silicon) is

$$\partial p'/\partial t = -p'/\tau_p + D_p \nabla^2 p' \tag{1}$$

where p' is the excess hole concentration to thermal equlibrium, τ_p is the hole lifetime, D_p is the hole diffusion coefficient. The solution of eq. (1) provides the transient of the hole excess in a unit of volume at a distance r from where the amount P_o of charges was created at $t = 0$

$$p'(t,r)dV = P_o \exp(-t/\tau_p)\exp(-r^2/4D_p t)/\left[8(\pi D_p t)^{3/2}\right] r^2\, dr\, d\Omega$$

where Ω is the solid angle. For an integration time[8] $\tau < \tau_p$ this equation becomes

$$p'(\tau,r)\,dV = P_o \exp(-r^2/2\sigma^2)/\left[(2\pi)^{3/2}\sigma^3\right] r^2\, dr\, d\Omega \tag{2}$$

where $\sigma = \sqrt{(2D_p\tau)}$. From eq. (2), we can calculate the probability that a charge created at a distance r from the actual position of the depleted region diffuses into it. One can show that i) only charges created up to a distance σ from the depleted region may migrate into it, and ii) the total amount of charges is $\approx (1/3)\sigma N$, where N is the number of h-e pairs created per unit length. The value of N is assumed to be constant over the distance σ. By considering an integration time of about $3\tau_t$ (namely ≈ 25 ns for a resistivity of $\approx 1500\ \Omega$cm), we have $\sigma \approx 24\ \mu$m. Thus only an equivalent region smaller than $\approx 8\ \mu$m in the field-free region contributes to the overall sensitive thickness of the detector.

The performance of a high-resistivity silicon detector operated as both fully depleted and undepleted device has been investigated by using a 30 GeV/c pion beam at

CERN-SPS[4]. At any applied voltage lower than that required for full depletion, the resulting sensed energy-straggling spectrum was in agreement with the energy-loss distribution[9] of a relativistic particle traversing a silicon absorber of thickness equal to the actual depleted layer.

In Figs. 1a and 1b, we show the energy-loss spectra of β^-s from a Ru source traversing a high-resistivity ($\approx$ 12500 Ωcm) detector operated at 7.5 V, and a low resistivity ($\approx$ 1500 Ωcm) detector operated at 60 V respectively. The depleted layers were $\approx$ 160 μm in both cases. The source was placed in front of the detector under investigation and the trigger formed for electrons crossing it and two downstream detectors. In this way only relativistic electrons, namely those with a kinetic energy between 1 and 3 MeV, were selected. Their most probable energy-loss, traversing $\approx$ 160 μm of silicon absorber, is $\approx$ 43 keV. The full width at half maxima, once subtracted the gaussian noise contribution, were 21.0 $\pm$ 3.0 keV and 18.2 $\pm$ 3.0 keV respectively.

2. 3. - Electronics for high-capacitance silicon detectors

In this section a relatively low-cost preamplifier, capable of working with detectors with capacitances up to 2600 pF, is presented. It is a charge-sensitive amplifier which delivers a voltage output for a time varying coulomb charge at its input. Its main purpose is to reduce the capacitative effect of undepleted silicon detectors. The dynamic range of 1000 is derived from the requirement of one to 1000 particles per event. The preamplifier (Fig. 2) was tested with a Mercury Pulse Generator, model PG-N-1, Elscint and since the shaping and amplifying stage is still in development, a Main Amplifier, Model CAV-N-1, Elscint (Fig. 3) has been used.

The required test-pulse amplitudes can be calculated from $E_{eq} = V_T C_T E_c q^{-1}$ where V_T is the test pulse, C_T the test capacitance + stray capacitance, E_{eq} the average energy-loss, E_c the conversion energy of silicon, and q the electron charge.

For C_T = 5 pF, E_c = 3.6 eV, E_{eq} = 50 keV and q = 1.6×10^{-19} Cb, for one particle per event is

$$V_{T_1} = 50 \text{ keV} \times 1.6 \times 10^{-19} / (3.6 \text{ eV} \times C_T) = 0.44 \text{ mV}$$

and for 1000 particles per event

$$V_{T_2} = 440 \text{ mV}.$$

Since the voltage gain depends on the feedback capacitance C_f, measurements were performed for both C_f = 1 pF and 5 pF.

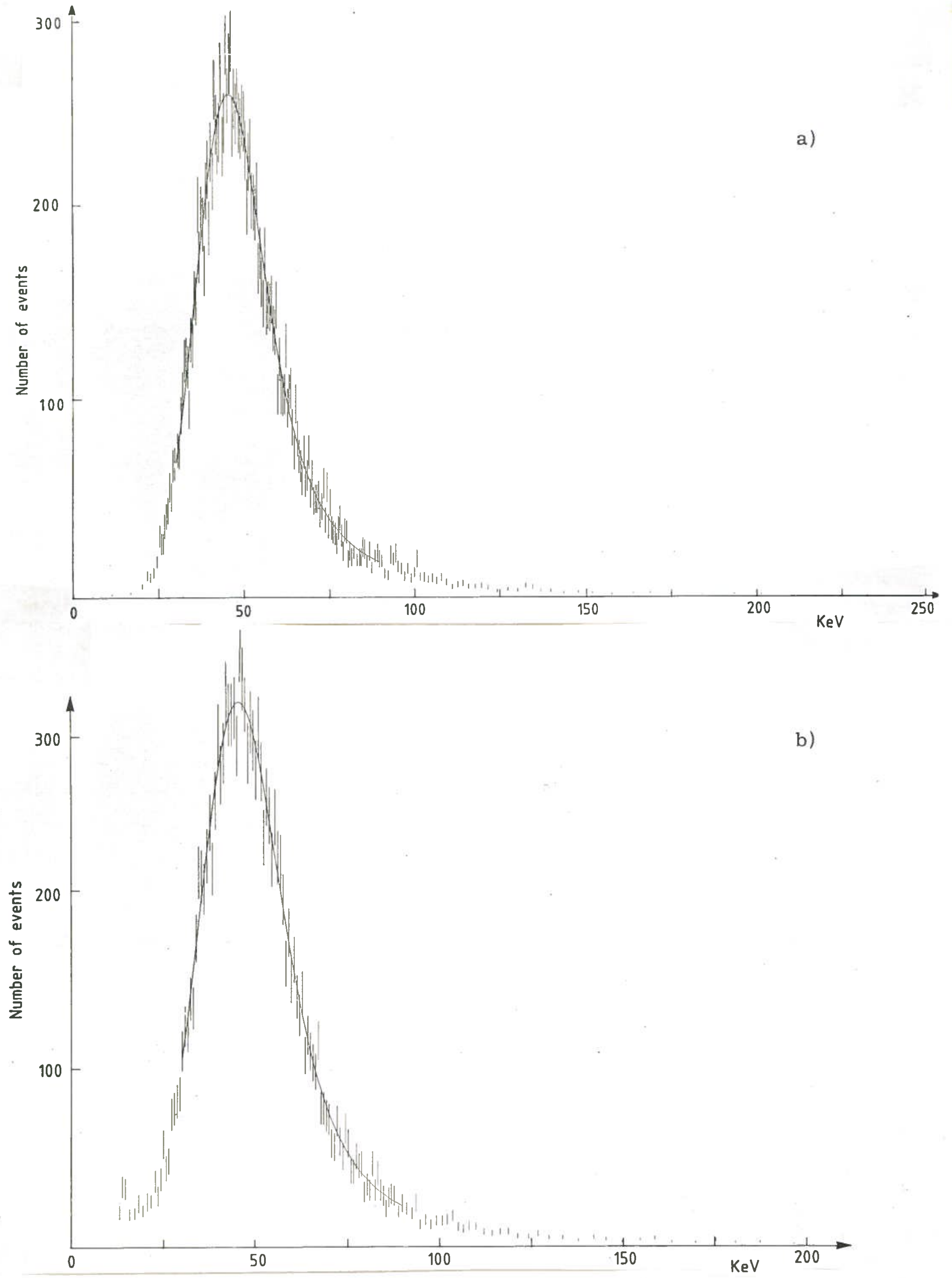

FIG. 1 - Energy-loss distribution of β^-s with kinetic energy between 1 and 3 MeV from a Ru source sensed by a) a high-resistivity ($\approx$ 12500 Ωcm) detector, b) a low-resistivity (1500 Ωcm) detector. The continuous lines are fits to the distributions. Both detectors were depleted up to $\approx$ 160 μm.

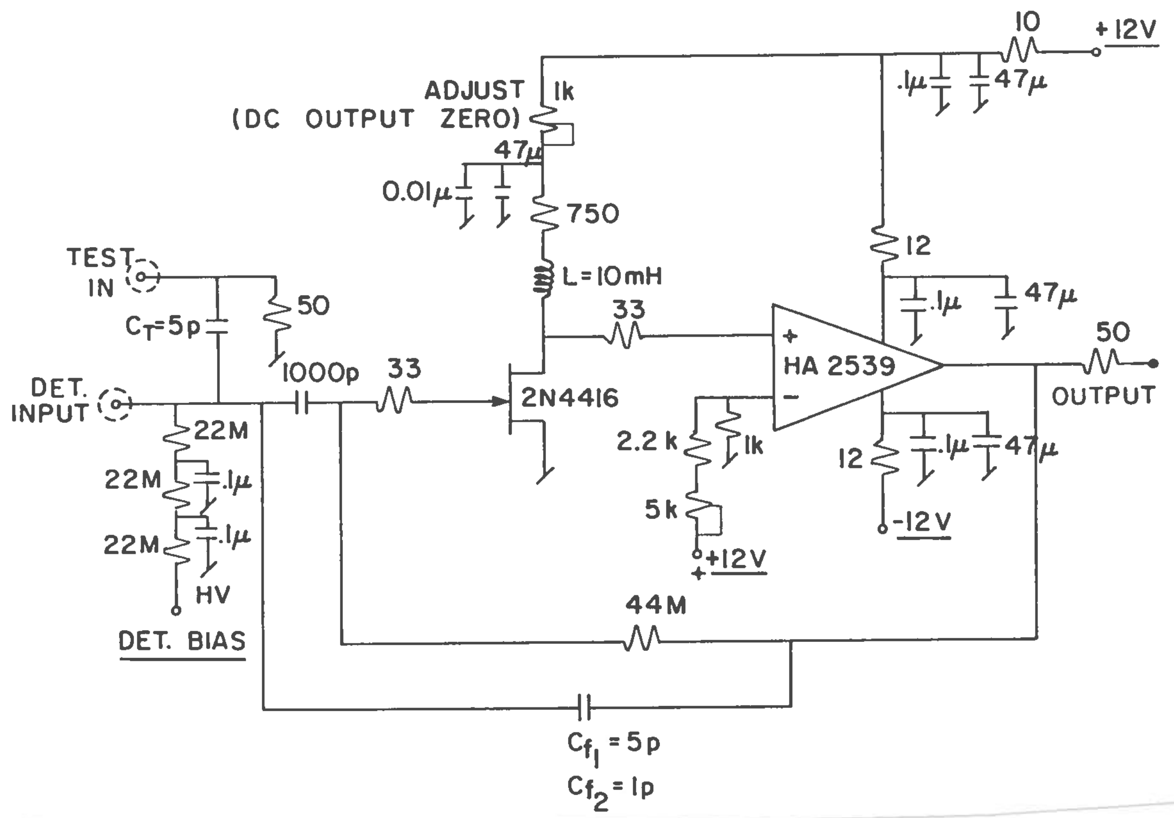

FIG. 2 - Charge-sensitive preamplifier.

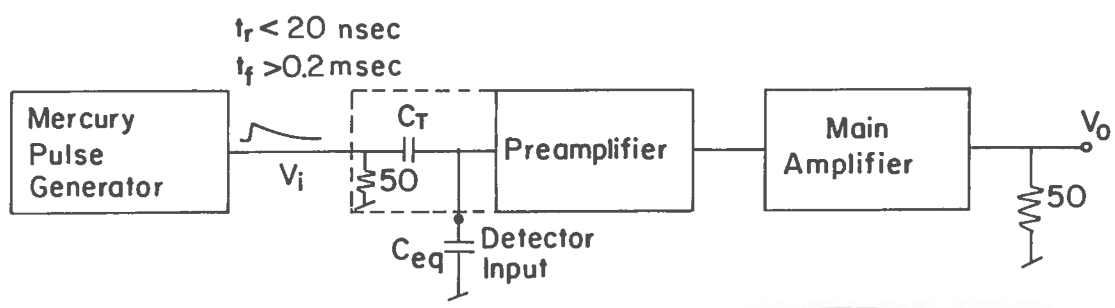

FIG. 3 - Experimental set-up of the preamplifier test.

As already mentioned the set-up of the measuring system (Fig. 3) consists of a Mercury pulse generator which feeds signals into the test-input of the preamplifier throught C_T (= 5 pF + stray capacitance). The output signals of the preamplifier are fed into the Main Amplifier which is set as follows:

time constant	= 0. 8 μs
Gain	= x 4
Noise (for C_{eq}=0)	= 2 mV.

The preamplifier was tested for linearity with no capacitance at the detector input and then for C_{eq} = 10-2620 pF.

A consideable improvement was achieved when an inductor was introduced at the positive input of the operational amplifier. Both the gain and noise performance improved but the amplifier can be used for C_{eq} greater than 100 pF since for smaller ones the circuit oscillates. This is obviously no problem since the preamplifier was designed to be used for high-capacitance detectors.

The preamplifier output signal is almost the same as input for C_f = 5 pF and about 5 times larger for C_f = 1 pF.

Results of the measurements for C_{eq} = 150 pF and C_T = 5 pF, for V_i = 200 mV and C_f = 5 pf, and for V_i = 200 mV and C_f = 1 pF, are presented in Tables I, II and III respectively.

TABLE I - Measurements for C_{eq} = 150 pF and C_T = 5 pF.

V_i (mV)	V_o (mV) C_f = 5 pF	V_o (mV) C_f = 1 pF
2	7	27
10	35	135
100	350	1350
200	700	2700
400	1400	----
Noise 2 mV		

TABLE II - Measurements for V_i = 200 mV and C_f = 5 pF.

C_{eq}	V_o (mV) without L	Noise (mV) p-p	V_o (mV) with L	Noise (mV) p-p
0	780	2	----	--
10	720	2	---	--
150	700	3.5	700	3
820	700	15	700	10
1800	690	35	700	20
2620	680	45	700	30

TABLE III - Measurements for V_i = 200 mV and C_f = 1 pF.

C_{eq}	V_o (mV) without L	Noise (mV) p-p	V_o (mV) with L	Noise (mV) p-p
0	2800	2	----	---
10	2800	2.5	----	---
150	2750	15	2800	7
820	2500	60	2600	40
1800	2100	90	2400	70
2620	1800	110	2200	100

The measurements were performed with the output of the preamplifier amplified by the Main Amplifier (Fig. 3). As seen from the results for a gain of 4 and a time constant of 0.8 μs the output voltage for C_f = 5 pF was about 750 mV, the maximum amplifier output would be 1.65 V. In order to obtain similiar output, a shaping and amplifying stage at the output of the preamplifier is currently being designed.

3. - THE LUMINOSITY MONITOR

The proposed luminosity monitor consists of a set of three doublets of microstrip detectors followed by a silicon/tungsten calorimeter.

The first plane in each doublet is a microstrip device with strips like anuli. The second one has radial strips. This way the direction of flight of the electron (or positron) is detected. The transversal resolution at a position x is given by the straight line fit

$$\sigma_x = \sigma\left[1/\Sigma w_i + (x - \langle x \rangle)^2/\Sigma w_i(x_i - \langle x \rangle)^2\right]^{1/2}$$

where σ is the transversal resolution of each detector, w_i are the weights attributed to each plane, $\langle x \rangle$ is the position of the centre of gravity of the detectors and x_i are their positions. As an example, for an interaction occuring at 8 m far from the microstrip set (sect. 3.1), a strip pitch of 200 μm and the doublets spaced by 9 cm, the value of σ_x turns out to be $\approx$ 1.3 cm.

The electron energy is measured by a sandwich consisting of 15 tungsten layers, the thickness of each being equivalent to two radiation lengths ($\approx$ 0.7 cm), interspaced by active 300 μm thick silicon sampling layers. Their resistivity is $\approx$ 1500 Ωcm and their depleted region (at 60 V) is $\approx$ 160 μm. The expected calorimeter energy resolution (sect. 2.1), assuming that the sampling fluctuations dominate, is

$$\sigma(E)/E = 13\%/\sqrt{(E)}\,.$$

3. 1. - Detector lay-out

As mentioned in section 1, the differential cross-section of Bhabha scattering at small angles is proportional to $(1/\theta^4)$. Thus the luminosity detector is to be located far from the interaction region and quite close to the beam line in order to detect electron scattered at very small angles. In Fig. 4, the luminosity monitor is positioned at about 8 m far from the interaction region and accepts electrons scattered at about 15 mr. Assuming a luminosity of 10^{31} cm^{-2}s^{-1} and a beam energy of 50 GeV, the rate of the detected elastic scattering events is about 10 s^{-1}. An elastic event is accepted when

i) the two reconstructed tracks are originated in the interaction region, and ii) the energies associated to either of them is consistent with the beam energy.

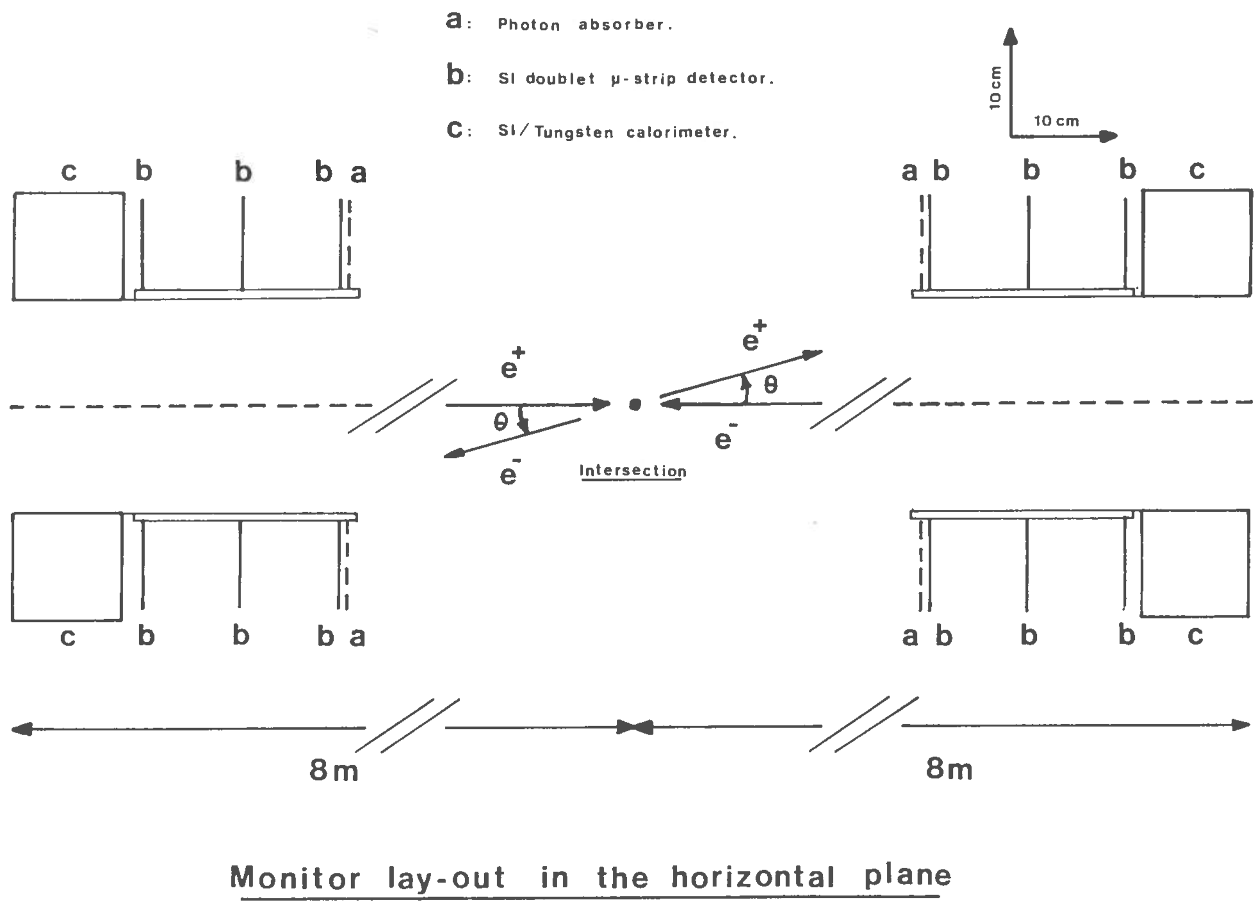

FIG. 4 - Luminosity monitor lay-out. A set of three microstrip doublets and a silicon/tungsten calorimeter are located at 8 m downstream the interaction region. A photon absorber is positioned in front of the detector.

When a low β quadrupole is located in front of the detector, one can exploit its defocusing property. Thus even smaller scattering angles are detected on one plane and the expected counting rate increases.

The main source of background in each detector is due to the synchrotron radiation generated in the upstream low β quadrupoles. As an example, the total photon flux for a beam of 1 mA and 50 GeV is about 1.8×10^{11} photons/bunch. They have energies up to 300 keV and centred around the critical energy $E_c \approx 120$ keV(10). Although a limited number of these photons ($\approx 10^3$) go towards the detector, a thin lead absorber ($\approx$ 0.1 radiation length) has to be placed in front of the microstrip detectord. This way both the photons and the subsequently emitted electrons are absorbed. The absorber does not affect the performance of the detector.

The background due to the beam-gas bremsstrahlung and off momentum particles are rejected by requiring that the two detected particles are in coincidence.

A prototype of the silicon/tungsten calorimeter will be tested at the X7 electron beam at CERN-SPS during the second half of 1983. It consists of 10 tungsten layers, each one of two radiation lengths and interspaced by a 5×5 cm^2 low resistivity (≈ 1500 Ωcm) silicon detector (Fig. 5) as active sampling device. The calorimeter, able to contain the full energy of a 50 GeV electron and with thinner passive layers, will be tested later on.

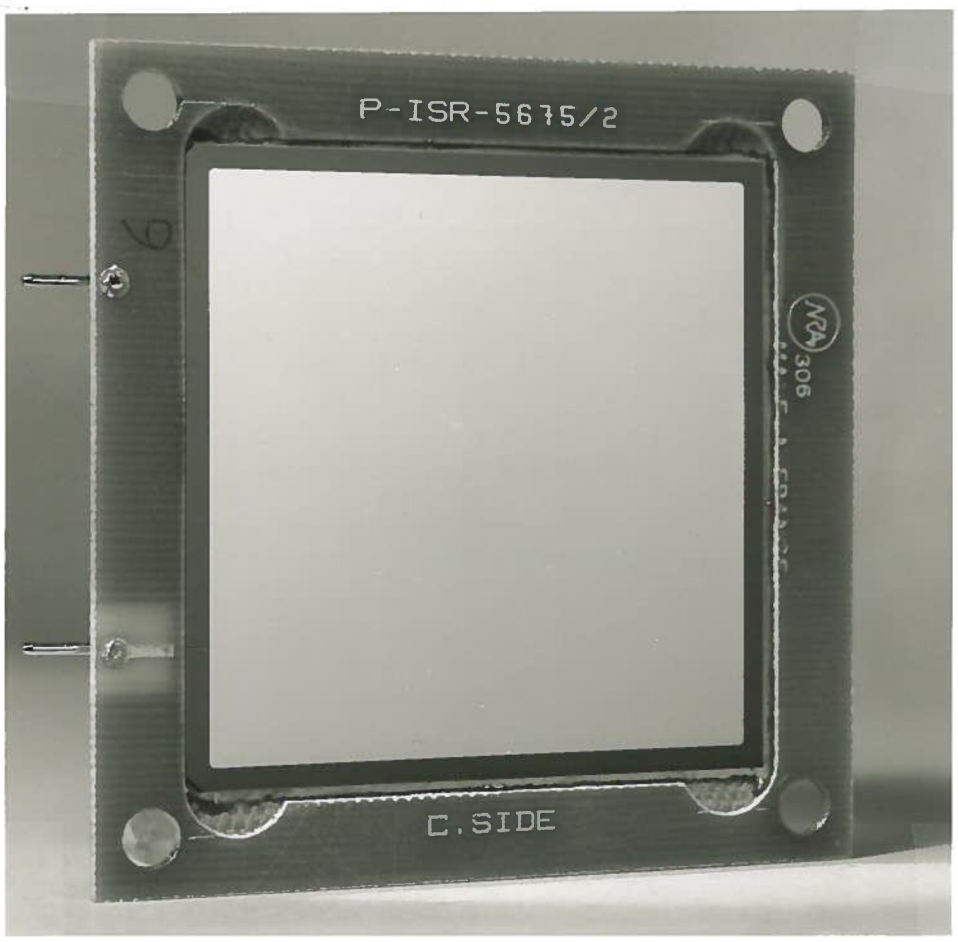

FIG. 5 - Silicon detector for active sampling layer of 5×5 cm^2 of active area.

3.2. - Radiation Damage

Recently, studies on radiation damage effects induced by relativistic particles have been carried out. Degraded operations, i.e. a strong increase of leakage current, were shown by ion-implanted detectors at fluence values greater than those required by surface-barrier devices(11). A more specific investigation on ion-implanted detector found that full charge collection is obtained by linearly increasing the voltage with fluence. In this way the detector could stand up to a fluence of $\ngtr 8.3 \times 10^{13}$ relativistic protons cm^{-2}, although a large disordered volume was estimated. Its effective size was explained by the fact that it is actually a region created by both the recoiling nucleus and the emitted nucleons and possibly enhanced by migration of vacancies(12).

Thousands of displacements can be created per high-energy hadronic interaction in silicon.

The most important absorption process in silicon for γ-rays between 60 keV and 15 MeV is due to Compton scattering. The recoil electrons are responsible for most of the damages. However in silicon the threshold of the electron kinetic energy to cause a displacement is about 250 keV. The probability that a single defect is produced by a γ-ray traversing 160 μm of silicon is about 1.6×10^{-4}. Thus, the synchrotron radiation photons radiated by the quadrupoles near the intersection region, whose energies are between 60 and 300 keV, are not expected to produce a strong radiation damage effect.

4. - CONCLUSION

Inexpensive low resistivity undepleted detectors can be applied in calorimetry as active sampling layers. Their sensitive region is defined by both the charge-depletion layer and few microns in the field-free region. The calorimeter energy resolution is only limited by the sampling fluctuations as a consequence of the higher silicon density compared with those ones of current active sampling devices.

A set of microstrip detectors followed by a silicon/tungsten calorimeter may provide a luminosity monitor appropriate to e^+e^- beam colliding machines. The possibility of installing the device close to the beam seems attractive due to the small detector volume then required.

Synchrotron radiated photons are not expected to cause any damage, thus to affect the performance of the luminosity monitor.

ACKNOWLEDGMENTS

Useful discussions with R. Klanner are gratefully acknowledged. The authors are indebted to the staff of the CERN E. A. group for their collaboration in preparing the forthcoming experimental tests.

REFERENCES AND FOOTNOTES

(1) - G. Barbiellini, F. Ceradini, L. Paoluzzi and R. Santonico, Nuclear Instr. and Meth. 123, 125 (1975).

(2) - P. G. Rancoita and A. Seidman, Riv. Nuovo Cimento 5, no. 7 (1982).

(3) - P. G. Rancoita, U. Koetz, R. Klanner and H. Lierl, Report of HERA Working Group on "Solid State Detectors", to appear in the Proceedings of the Workshop on Experimentation on HERA Machine, Amsterdam, 9-12 June 1983, under publication.

(4) - G. Barbiellini and P. G. Rancoita, A luminosity monitor for LEP using electromagnetic calorimeters: the silicon/lead sandwich, CERN-EP Internal Report 83-01 (1983).

(5) - The calorimeter length, L, in unit of radiation lengths is

$$L(98\%) = \lambda t_{med}$$

where $t_{med} = [\ln(E/\varepsilon)+a]$ (a = 0.4 or 1.2 for electrons or gammas), E is the incoming energy, ε is the critical energy and λ is between 2.6 and 3.0.

(6) - U. Amaldi, Physica Scripta 23, 408 (1981).

(7) - The carrier-diffusion length for holes, which are the minority carriers in the n-type silicon, is defined as

$$L_p = (D_p \tau_p)^{1/2}$$

where D_p is the diffusion coefficient for holes $kT\mu_h/e$, where k is the Boltzman constant, T is the absolute temperature, μ_h is the hole mobility and τ_p is the hole lifetime.

(8) - The integration time is the time during which the charge from the detector is integrated.

(9) - S. Hancock, F. James, J. Movchet, P. G. Rancoita and L. Van Rossum, Phys. Rev. A28, 615 (1983).

(10) - P. Roudeau, O. Leistam and K. Potter, A simple method to study the backscattering of synchrotron radiation around an interaction region at LEP, LEP note 439 (1983).

(11) - E. Heijne, Radiation Damage: Experience with silicon detectros in high-energy beams at CERN, Report CERN EF-BEAM 81-6 (1981).

(12) - P. Borgeaud, G. McEwen, P. G. Rancoita and A. Seidman, Nuclear Instr. and Meth. 211, 363 (1983).